Nuclear Forward Scattering of Synchrotron Radiation by ^{99}Ru

D. Bessas,[1,*] D. G. Merkel,[1] A. I. Chumakov,[1] R. Rüffer,[1] R. P. Hermann,[2,3] I. Sergueev,[4]
A. Mahmoud,[2] B. Klobes,[2] M. A. McGuire,[5] M. T. Sougrati,[6,7] and L. Stievano[6,7]

[1]*European Synchrotron Radiation Facility, F-38043 Grenoble, France*
[2]*Jülich Centre for Neutron Science, JCNS, and Peter Grünberg Institut PGI, JARA-FIT,
Forschungszentrum Jülich GmbH, D-52425 Jülich, Germany*
[3]*Faculté des Sciences, Université de Liège, B-4000 Liège, Belgium*
[4]*Deutsches Elektronen-Synchrotron, D-22607 Hamburg, Germany*
[5]*Material Science and Technology Division, Oak Ridge National Laboratory, Oak Ridge, Tennessee 37831, USA*
[6]*Institute Charles Gerhard AIME UMR CNRS 5253, Université Montpellier 2, F-34095 Montpellier, France*
[7]*Réseau sur le Stockage Electrochimique de l'Energie (RS2E), FR CNRS 3459, France*

We measured nuclear forward scattering spectra utilizing the ^{99}Ru transition, 89.571(3) keV, with a notably mixed $E2/M1$ multipolarity. The extension of the standard evaluation routines to include mixed multipolarity allows us to extract electric and magnetic hyperfine interactions from ^{99}Ru-containing compounds. This paves the way for several other high-energy Mössbauer transitions, $E \sim 90$ keV. The high energy of such transitions allows for *operando* nuclear forward scattering studies in real devices.

Nuclear forward scattering of synchrotron radiation [1,2] is nowadays a standard technique for obtaining information similar to that extracted from Mössbauer spectroscopy [3]. This technique is particularly useful when preparation of the radioactive source for Mössbauer spectroscopy is difficult, when the lifetime of the radioactive source is short, or when the experimental setup requires a collimated or small-size beam.

Synchrotron radiation matching the energy difference between the nuclear ground state and an excited state impinges on the sample and leads to nuclear excitation. The excited state has a finite lifetime, and the resonantly scattered photons are delayed with respect to nonresonantly scattered (prompt) photons. Both coherent nuclear forward scattering [4] and incoherent fluorescence are observed. The typical lifetime of excited states ranges between 0.2 and 200 ns and matches the bunch structure of the current synchrotron radiation facilities. Hence, the nuclear forward scattering can, in principle, be measured for any of the Mössbauer isotopes.

The typical bandwidth of conventional x-ray optics is in the eV range. As a result, every photon resonantly scattered is accompanied by between 10^6 and 10^9 photons that are not nuclearly scattered, often overloading the detection scheme [5,6]. In order to circumvent detection overload from nonresonant quanta, monochromatization of the x-ray beam by high-resolution monochromators with meV bandpass [7] is typically used. Such monochromators are usually made out of silicon. Efficient high-resolution monochromatization for energies above 30 keV is restricted because of the physical properties of silicon (see Ref. [8]), thus, seriously limiting the number of high-energy Mössbauer transitions studied using synchrotron radiation.

Other approaches were suggested to circumvent the pitfalls of silicon monochromators and, thus, the problem of nonresonant detection overload, such as sapphire back-scattering monochromatization [9–12] and nuclear light-house effect [13]. However, these approaches seriously limit the sample environment.

It was previously shown that nuclear forward scattering around 70 keV can be carried out with medium-resolution monochromatization of 30 meV [14] or even 100 meV [12]. The extension of this concept to higher energies in combination with an optimized detector system and the lower flux of synchrotron radiation above 80 keV highly reduces the need for sophisticated approaches to circumvent nonresonant detection overload. In addition, the high energy allows for *operando* measurements in real devices.

Although conventional Mössbauer spectroscopy can be applied to high-energy Mössbauer transitions such as ^{155}Gd [60.0106(6) keV] and ^{166}Er [80.577(2) keV], nuclear forward scattering with a collimated small-size beam by ^{156}Gd [88.970(1) keV] and ^{164}Er [91.38(2) keV] may provide superior information related to hyperfine interactions on nanostructures and under extreme conditions, e.g., the study of magnetic anisotropies in Gd nanostructures [15] and studies of partial amorphization of Er_2O_3 under applied pressure [16]. Moreover, a study of a yet unexplored chemistry related to the novel electronic properties of hafnium compounds such as two-dimensional hafnium honeycombs—similar to graphene—structure [17], hafnium carbides for use in extreme environments [18], and studies related to the applications of hafnium hydride in nuclear power plants [19] are now feasible by nuclear forward scattering on ^{176}Hf [88.349(24) keV].

In this Letter, we report on nuclear forward scattering (NFS) of synchrotron radiation at energy as high as 90 keV using a conventional double-crystal monochromator and a multielement avalanche photodiode (APD) detector. Using such a setup, we measured (in two hours each) nuclear forward scattering spectra for ^{99}Ru metal and ^{99}RuO$_2$ 99% enriched to ^{99}Ru and (in ten hours) spectra for SrRuO$_3$ [20,21] with 12.7% ^{99}Ru natural abundance [22]. The related information, i.e., absolute values of recoil-free fraction (f_{LM}), its temperature dependence, and the related Debye temperature in ^{99}Ru metal and the quadrupole splitting in ^{99}RuO$_2$ as well as the hyperfine magnetic field in SrRuO$_3$ is extracted by extending the available routines including the mixture of $E2$ and $M1$ multipolarity.

^{99}Ru has a nuclear ground state with spin $I_g = 5/2$ and the first excited state with spin $I_e = 3/2$. The nuclear transition occurs via a combination of electric quadrupole $E2$ and magnetic dipole $M1$ radiation with a mixing ratio $\delta^2 = 2.7(6)$ [23]. The Mössbauer effect in ^{99}Ru was first observed by Kistner *et al.* [24]. Several groups [25–29] have worked on extracting hyperfine interaction parameters in Ru-based compounds. The half-life, only 16 days, of the used ^{99}Rh radioactive source and the necessity to produce it using a particle accelerator limits the applicability of ^{99}Ru Mössbauer spectroscopy. However, currently there is high demand for hyperfine interaction studies in Ru-containing compounds with various applications, i.e., photocontrolled DNA binding in life sciences [30], energy harvesting using photovoltaic cells [31], and energy storage in lithium-ion batteries [32].

The experiment was carried out at the Nuclear Resonance beamline ID18 [33] of the European Synchrotron Radiation Facility. The storage ring was operating in 16-bunch mode providing 176 ns interbunch spacing. The optical elements in the experimental setup were a compound refractive lense (CRL) [34] for collimation comprised of 115 cylindrical holes of 1 mm diameter in beryllium, with 50% transmission at 90 keV, and a Si (3 3 3) double-crystal monochromator [see Fig. 1(a)]. The internal conversion, with coefficient 1.50(3) [35], converts the delayed resonant quanta to delayed incoherent Ru K_a fluorescence at 19.279 keV which is easier to detect [36]. The nuclear transition energy E_0 for the ^{99}Ru first excited state was determined by measuring the delayed K_a fluorescence coming from a ^{99}Ru metal sample placed 3 mm away from a 100 mm^2, 100 μm thick, APD [see Fig. 1(a)]. The estimated efficiency of the Si APD used for 19 keV is ~10%. The energy resolution of the Si (3 3 3) double-crystal monochromator measured by the delayed Ru K_a fluorescence is shown in Fig. 1(b). This energy resolution is defined by the angular spread of the beam after CRL. A typical angular spread is given by the full width at half maximum, 3.6(1) μrad, of a Gaussian function fitted to the experimental data. The angular acceptance of the Si (3 3 3) monochromator is 0.53 μrad. Thus, the monochromator
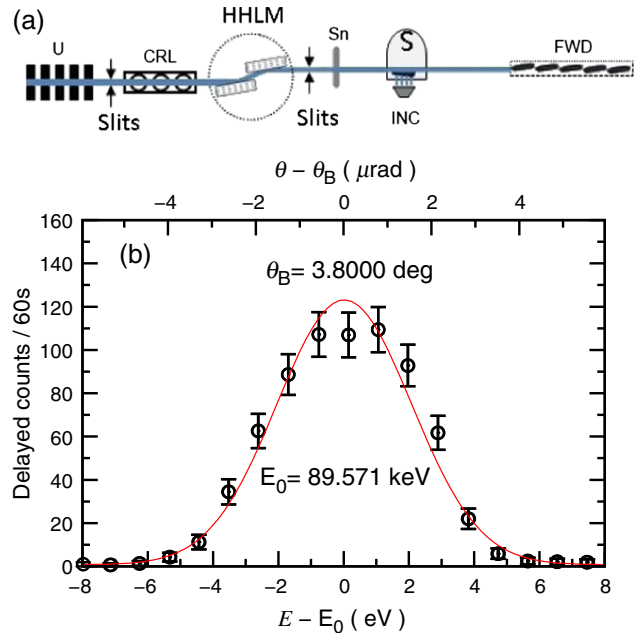

FIG. 1 (color online). (a) The experimental setup consisted of three undulators (U), two pairs of slits, a compound refractive lense (CRL) for collimation, a Si (3 3 3) double-crystal monochromator (HHLM), a Sn absorber (see text), the sample (S) in a helium cryostat, a Si APD for measuring the Ru K_a fluorescence (INC), and the ten-element Si APD for measuring the nuclear forward scattering (FWD). (b) The energy resolution of the Si (3 3 3) double-crystal monochromator measured by the delayed Ru K_a fluorescence. The angular spread of the beam after CRL is also shown (upper tics). The line is a fit with a Gaussian function to the experimental data with 3.6(1) μrad full width at half maximum.

accepts only ~15% of the beam. The time spectra of the nuclear forward scattering were recorded by using a ten-element array consisting of 30 μm thick, 3 mm diameter Si APD with time resolution of ~0.5 ns. All detection elements are inclined and displaced vertically with respect to each other in order to cover the full beam height, 0.5 mm, and to equally distribute the radiation load. The thickness of each element along the beam was ~2.5 mm, resulting in a detection efficiency of ~10% at 89 keV. The photon flux detected by each APD in this detection scheme was less than 2×10^6 photons/s at 70 mA storage ring current, far from the saturation regime. The detected background of 0.03 Hz measured 20 eV away from the resonant energy is uniformly distributed in time (see Fig. 2). A slight increase around 2 ns could be attributed to scattering of the beam in the detector housing. A similar detector is presented in Ref. [37].

The double-crystal monochromator allows transmission for radiation related both to the third harmonic—Si (3 3 3)— with energy of 89.6 keV, and the first harmonic—Si (1 1 1)—with energy of 29.9 keV. The coexistence of the first and third harmonic gave us the opportunity to calibrate the energy scale using the Sn K edge (29.2004(2) keV [38]).
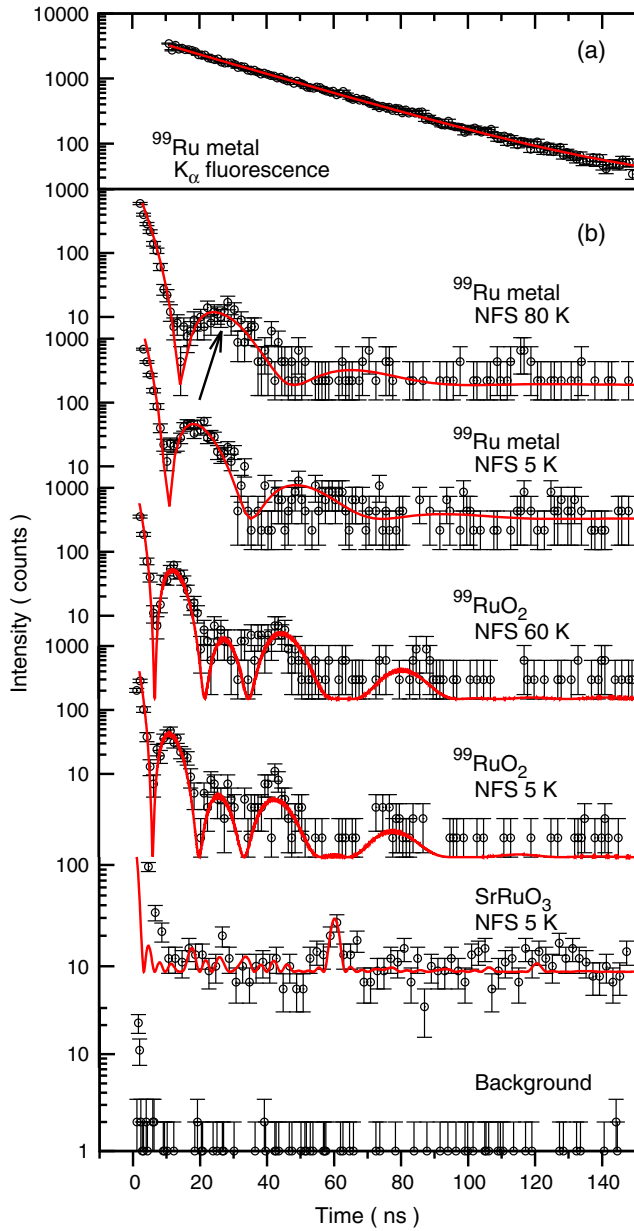
FIG. 2 (color online).   (a) The time distribution of the delayed incoherent Ru K_a fluorescence obtained on ^{99}Ru metal. (b) The nuclear forward scattering obtained on ^{99}Ru metal at 5 and 80 K (2 h each), the spectra obtained on ^{99}RuO$_2$ at 5 and 60 K (2 h each), respectively, the spectra obtained on SrRuO$_3$ at 5 K (10 h), and a measurement of the background 20 eV away from resonance (0.5 h). Solid lines show the fit of the experimental data (see text). The arrow between 5 and 80 K at the ^{99}Ru-metal data highlights the stretching in the dynamical beats due to the reduction in effective thickness.

The resonance energy for the ^{99}Ru first excited state was found to be 89.571(3) keV, in excellent agreement with the tabulated value, 89.57(6) keV [39]. In order to avoid detector overload in the forward direction, the 29.9 keV radiation was filtered out by a 200 μm Sn foil [40]. The small fraction of low-energy radiation passing through the Sn foil

is further absorbed by the ruthenium-containing sample, 3.5 mg/mm^2 of ^{99}Ru.

The recorded time distribution of the delayed Ru K_a fluorescence reveals an exponential decay [see Fig. 2(a)]. Fitting the data with a simple exponential function $I(t) = I_0 e^{-t/t_0} + c$ yields a lifetime t_0 of the excited state of 28.8(3) ns. The lifetime extracted herein is in agreement with the reported value of 29(1) ns [41] measured using the delayed coincidence technique.

The nuclear forward spectrum recorded by ^{99}Ru metal at 5 and 80 K with $\sim$0.5 Hz count rate indicates a pronounced structure [see Fig. 2(b)]. The beat pattern broadens and shifts in time when the temperature increases. In ^{99}Ru metal, no electric or magnetic hyperfine splitting is present [42]. In this case, the nuclear forward scattering intensity is given by Kagan *et al.* [43]. In order to extract the recoil-free fraction from the obtained spectrum, the unitless effective thickness ξ of the sample is used:

$$\xi = \frac{1}{4} L \sigma_0 f_{LM} \frac{\beta}{V_{Ru}}, \qquad (1)$$

where L is the geometric sample thickness, σ_0 is the nuclear resonant absorption cross section, f_{LM} is the recoil-free fraction known as the Lamb-Mössbauer factor, β is the isotopic enrichment, and V_{Ru} is the volume per Ru atom. Pronounced beating, i.e., dynamical beats, is observed when ξ is large. The spectra for ^{99}Ru metal shown in Fig. 2(b) were fitted between 5 and 150 ns, and the obtained ξ is 10.01(9) and 7.35(6) at 5 and 80 K, respectively. The f_{LM} and the Debye temperature are extracted by fitting a Debye model to the obtained values of the effective thickness [12]. The obtained f_{LM} are 0.19(1) and 0.14(1) at 5 and 80 K, respectively, and the obtained Debye temperature is 466(50) K. The Debye temperature extracted herein is in good agreement with the Debye temperature 495(24) K extracted from x-ray diffraction on Ru [44,45].

The mixing of electric quadrupole and magnetic dipole multipolarity of the nuclear transition is not included in the available fitting routines [46,47], and, as a result, they cannot be used to analyze our measurements on ^{99}RuO$_2$ and SrRuO$_3$. Thus, we had to modify [48] the available routines for extracting the quadrupole splitting and the magnetic hyperfine field in paramagnetic ^{99}RuO$_2$ and ferromagnetic SrRuO$_3$, respectively. The fit of the data was performed with an algorithm [14] developed on the basis of the Fourier transformation of the energy spectrum to nuclear forward scattering [43] and extended for the case of large effective thickness. The mixing of $E2$ and $M1$ multipolarities was included with a fixed ratio $\delta^2(E2/M1) = 2.7$ [23]. The ratio of the nuclear quadrupole moments of the ground Q_g and excited state Q_e were fixed to $Q_e/Q_g = 2.93$ [52]. The nuclear magnetic moments of the ground state $\mu_g = -0.641 \mu_n$ and of the excited state

$\mu_e = -0.284\mu_n$ were also fixed. The spectra were treated using an isotropic distribution of the hyperfine interactions.

The beats in the NFS spectra of $^{99}RuO_2$ are due to a combination of the dynamical beats related to the large effective thickness and the quantum beats related to the quadrupole interaction which merge into hybrid beats [53]. By using the routine we developed, we fitted the data with only two free parameters: the quadrupole splitting $eQ_e V_{zz}/2$ and the effective thickness. The obtained quadrupole splitting $5.93(15)\,\Gamma_0$ or 0.44(1) mm/s agrees with that obtained by Mössbauer spectroscopy, 0.5(1) mm/s [42]. The f_{LM} and the Debye temperature are extracted similarly to the ^{99}Ru-metal case. The obtained Lamb-Mössbauer factors are 0.24(1) and 0.22(1) at 5 and 60 K, respectively, and the extracted Debye temperature is 535(60) K. This value is slightly lower than the Debye temperature measured previously using calorimetry [54], 610(10) K at 10 K.

The shape of the nuclear forward scattering spectrum of $SrRuO_3$ is defined by the magnetic hyperfine splitting. The obtained count rate was low, 0.04 Hz, and comparable with the background count rate. The low count rate is due to the low ^{99}Ru natural isotopic abundance. Magnetic splitting of the excited and ground state for the $E2/M1$ mixed multipolarity allows for 18 transitions. Because of the numerous transitions, distinct peaks appear in the nuclear forward spectrum. A similar effect was observed for the ^{181}Ta nuclear transition [55]. In the case of $SrRuO_3$, the clearly seen peak at 60 ns [see Fig. 2(b)] allows us to precisely extract a hyperfine magnetic field of 33.9(5) T at 5 K. This value is in agreement with the result 33.0(4) T at 4 K determined by Mössbauer spectroscopy measurements [56,57].

In conclusion, we have studied the nuclear forward scattering by the 89.571(3) keV in several ^{99}Ru-containing reference materials, i.e., ^{99}Ru metal, $^{99}RuO_2$, and $SrRuO_3$. Moreover, we have modified the available fitting routines for extracting electric and magnetic hyperfine interaction in mixed multipolarity transitions. The typical count rate observed on the ^{99}Ru-enriched sample was ∼0.5 Hz and allows us to acquire reasonable statistics in two hours. Measurements on non-^{99}Ru-enriched samples are currently challenging. The observed count rate can be increased in the future by at least an order of magnitude by optimization and upgrading the optics and the detector. Under such conditions, measurements on nonenriched samples will be feasible. By taking advantage of the high penetration depth of the radiation at 89 keV [58] as well as of the simplicity of the experimental setup *operando* hyperfine interaction, studies on real devices are now feasible. Our study opens a new field of research not only on ruthenium compounds with a variety of application, i.e., photocontrolled DNA binding in life sciences [30], energy harvesting using photovoltaic cells [31], energy storage in lithium-ion batteries [32], and ruthenium catalyst systems [59], but also on isotopes which have similar nuclear transition

energies, ^{176}Hf [88.349(24) keV], ^{156}Gd [88.970(1) keV], and ^{164}Er [91.38(2) keV]. Despite the expectedly low f_{LM} in organometallic compounds, feasibility measurements on ruthenium nitrosyls already exist in the literature [60] using conventional Mössbauer spectroscopy.

[*] bessas@esrf.fr

[1] J. B. Hastings, D. P. Siddons, U. van Bürck, R. Hollatz, and U. Bergmann, Phys. Rev. Lett. **66**, 770 (1991).

[2] U. van Bürck, D. P. Siddons, J. B. Hastings, U. Bergmann, and R. Hollatz, Phys. Rev. B **46**, 6207 (1992).

[3] P. Gütlich, E. Bill, and A. X. Trautwein, *Mössbauer Spectroscopy and Transition Metal Chemistry: Fundamentals and Applications* (Springer, New York, 2011).

[4] A. Q. R. Baron, A. I. Chumakov, H. F. Grünsteudel, H. Grünsteudel, L. Niesen, and R. Rüffer, Phys. Rev. Lett. **77**, 4808 (1996).

[5] A. Q. Baron, Hyperfine Interact. **125**, 29 (2000).

[6] E. Gerdau, Hyperfine Interact. **90**, 301 (1994).

[7] T. Toellner, Hyperfine Interact. **125**, 3 (2000).

[8] Y. V. Shvyd'ko, *X-Ray Optics: High Energy-Resolution Applications* (Springer, New York, 2004).

[9] H.-C. Wille, R. P. Hermann, I. Sergueev, U. Pelzer, A. Möchel, T. Claudio, J. Perß on, R. Rüffer, A. Said, and Y. Shvyd'ko, Europhys. Lett. **91**, 62001 (2010).

[10] H.-C. Wille, Y. V. Shvyd'ko, E. E. Alp, H. D. Rüter, O. Leupold, I. Sergueev, R. Rüffer, A. Barla, and J. P. Sanchez, Europhys. Lett. **74**, 170 (2006).

[11] B. Klobes, A. Desmedt, I. Sergueev, K. Schmalzl, and R. P. Hermann, Europhys. Lett. **103**, 36001 (2013).

[12] R. E. Simon, I. Sergueev, J. Persson, C. A. McCammon, F. Hatert, and R. P. Hermann, Europhys. Lett. **104**, 17006 (2013).

[13] R. Röhlsberger, T. S. Toellner, W. Sturhahn, K. W. Quast, E. E. Alp, A. Bernhard, E. Burkel, O. Leupold, and E. Gerdau, Phys. Rev. Lett. **84**, 1007 (2000).

[14] I. Sergueev, A. I. Chumakov, T. H. Deschaux Beaume-Dang, R. Rüffer, C. Strohm, and U. van Bürck, Phys. Rev. Lett. **99**, 097601 (2007).

[15] C.-J. Hsu, S. V. Prikhodko, C.-Y. Wang, L.-J. Chen, and G. P. Carman, J. Appl. Phys. **111**, 053916 (2012).

[16] X. Ren, X. Yan, P. Wang, Y. Li, S. Wang, F. Peng, L. Xiong, J. Liu, and D. He, High Press. Res. **34**, 70 (2014).

[17] L. Li, Y. Wang, S. Xie, X.-B. Li, Y.-Q. Wang, R. Wu, H. Sun, S. Zhang, and H.-J. Gao, Nano Lett. **13**, 4671 (2013).

[18] Q. Zeng, J. Peng, A. R. Oganov, Q. Zhu, C. Xie, X. Zhang, D. Dong, L. Zhang, and L. Cheng, Phys. Rev. B **88**, 214107 (2013).

[19] K. Konashi and M. Yamawaki, Adv. Appl. Ceram. **111**, 106 (2012).

[20] A. Callaghan, C. W. Moeller, and R. Ward, Inorg. Chem. **5**, 1572 (1966).

[21] J. M. Longo, P. M. Raccah, and J. B. Goodenough, J. Appl. Phys. **39**, 1327 (1968).

[22] $SrRuO_3$ was synthesized by heating a mixture of $SrCO_3$ and Ru powders at $1000\,°C$. X-ray diffraction confirmed that the product was single phase $SrRuO_3$ (space group Pnma), and magnetization measurements showed the expected Curie temperature near 160 K.

[23] O. C. Kistner, Phys. Rev. **144**, 1022 (1966).

[24] O. Kistner, S. Monaro, and R. Segnan, Phys. Lett. **5**, 299 (1963).

[25] T. C. Gibb, R. Greatrex, N. N. Greenwood, and P. Kaspi, J. Chem. Soc. D **1971**, 319 (1971).

[26] M. De Marco, D. Graf, J. Rijssenbeek, R. J. Cava, D. Z. Wang, Y. Tu, Z. F. Ren, J. H. Wang, M. Haka, S. Toorongian *et al.*, Phys. Rev. B **60**, 7570 (1999).

[27] W. Potzel, F. Wagner, R. Mössbauer, G. Kaindl, and H. Seltzer, Z. Phys. **241**, 179 (1971).

[28] D. C. Foyt, M. Good, J. Cosgrove, and R. Collins, J. Inorg. Nucl. Chem. **37**, 1913 (1975).

[29] Y. Kobayashi, J. Phys. Conf. Ser. **217**, 012023 (2010).

[30] F. Barragán, P. López-Senín, L. Salassa, S. Betanzos-Lara, A. Habtemariam, V. Moreno, P. J. Sadler, and V. Marchán, J. Am. Chem. Soc. **133**, 14098 (2011).

[31] T. Kinoshita, J. T. Dy, S. Uchida, T. Kubo, and H. Segawa, Nat. Photonics **7**, 535 (2013).

[32] M. Sathiya, G. Rousse, K. Ramesha, C. P. Laisa, H. Vezin, M. T. Sougrati, M.-L. Doublet, D. Foix, D. Gonbeau, W. Walker *et al.*, Nat. Mater. **12**, 827 (2013).

[33] R. Rüffer and A. I. Chumakov, Hyperfine Interact. **97–98**, 589 (1996).

[34] A. Snigirev, V. Kohn, I. Snigireva, and B. Lengeler, Nature (London) **384**, 49 (1996).

[35] T. Kibédi, T. W. Burrows, M. B. Trzhaskovskaya, P. M. Davidson, and C. W. Nestor, Jr., Nucl. Instrum. Methods Phys. Res., Sect. A **589**, 202 (2008).

[36] M. Seto, R. Masuda, S. Higashitaniguchi, S. Kitao, Y. Kobayashi, C. Inaba, T. Mitsui, and Y. Yoda, Phys. Rev. Lett. **102**, 217602 (2009).

[37] A. Q. R. Baron, S. Kishimoto, J. Morse, and J.-M. Rigal, J. Synchrotron Radiat. **13**, 131 (2006).

[38] S. Kraft, J. Stümpel, P. Becker, and U. Kuetgens, Rev. Sci. Instrum. **67**, 681 (1996).

[39] E. Browne and J. Tuli, Nucl. Data Sheets **112**, 275 (2011).

[40] The transmission of the 29.9 and the 89.6 kev radiation is 0.2% and 72%, respectively.

[41] O. C. Kistner, S. Monaro, and A. Schwarzschild, Phys. Rev. **137**, B23 (1965).

[42] G. Kaindl, W. Potzel, F. Wagner, U. Zahn, and R. Mössbauer, Z. Phys. **226**, 103 (1969).

[43] Y. Kagan, A. M. Afanas'ev, and V. G. Kohn, J. Phys. C **12**, 615 (1979).

[44] D. Singh and Y. P. Varshni, Acta Crystallogr., Sect. A: Cryst. Phys., Diffr., Theor. Gen. Crystallogr. **38**, 854 (1982).

[45] M. Shankar Narayana, N. Gopi Krishna, and D. B. Sirdeshmukh, Acta Crystallogr. Sect. A **57**, 217 (2001).

[46] Y. Shvyd'ko, Hyperfine Interact. **125**, 173 (2000).

[47] W. Sturhahn, Hyperfine Interact. **125**, 149 (2000).

[48] See Supplemental Material at http://link.aps.org/supplemental/10.1103/PhysRevLett.113.147601, which includes Refs. [43,49–51], for deriving the nuclear resonant absorption amplitude in the time domain for mixed multi-polarity transitions.

[49] M. Blume and O. C. Kistner, Phys. Rev. **171**, 417 (1968).

[50] D. A. Varshalovich, A. N. Moskalev, and V. K. Khersonskii, *Quantum Theory of Angular Momentum* (World Scientific, Singapore, 1988).

[51] R. Steffen and K. Alder, in *The Electromagnetic Interaction in Nuclear Spectroscopy*, edited by W. Hamilton (North-Holland, Amsterdam, 1975), pp. 505–583.

[52] O. C. Kistner and A. H. Lumpkin, Phys. Rev. C **13**, 1132 (1976).

[53] Y. V. Shvyd'ko, U. van Bürck, W. Potzel, P. Schindelmann, E. Gerdau, O. Leupold, J. Metge, H. D. Rüter, and G. V. Smirnov, Phys. Rev. B **57**, 3552 (1998).

[54] B. C. Passenheim and D. C. McCollum, J. Chem. Phys. **51**, 320 (1969).

[55] O. Leupold, A. Chumakov, E. Alp, W. Sturhahn, and A. Baron, Hyperfine Interact. **123–124**, 611 (1999).

[56] M. DeMarco, G. Cao, J. E. Crow, D. Coffey, S. Toorongian, M. Haka, and J. Fridmann, Phys. Rev. B **62**, 14297 (2000).

[57] T. C. Gibb, R. Greatrex, N. N. Greenwood, D. C. Puxley, and K. G. Snowdon, J. Solid State Chem. **11**, 17 (1974).

[58] At 89 keV, 2 mm of steel has 50% transmission.

[59] C. A. Clausen III and M. L. Good, in *Mössbauer Effect Methodology*, edited by I. Gruverman and C. Seidel (Springer, New York, 1976), pp. 93–118.

[60] M. S. Goodman, M. J. DeMarco, M. S. Haka, S. A. Toorongian, and J. Fridmann, J. Chem. Soc. Dalton Trans. **2002**, 117, (2002).